Bull. Chem. Soc. Ethiop. **2024**, 38(3), 725-738. ISSN 1011-3924

Printed in Ethiopia
DOI: https://dx.doi.org/10.4314/bcse.v38i3.14 Online ISSN 1726-801X

SYNTHESIS, SPECTROSCOPIC AND BIOLOGICAL CHARACTERIZATIONS OF PLATINUM(IV), RUTHENIUM(III) AND IRIDIUM(III) THEOPHYLLINE COMPLEXES

Abeer A. El-Habeeb[1] and Moamen S. Refat[2*]

[1]Department of Chemistry, College of Science, Princess Nourah bint Abdulrahman University, P.O. Box 84428, Riyadh 11671, Saudi Arabia
[2]Department of Chemistry, College of Science, Taif University, P.O. Box 11099, Taif 21944, Saudi Arabia

(Received February 5, 2024; Revised February 23, 2024; Accepted February 27, 2024)

ABSTRACT. This study used micro-analyses, (FTIR, UV-Vis) spectra, magnetic, thermogravimetric, X-ray powder diffraction (XRD) patterns, and transmittance electron microscopy (TEM) techniques to characterize three synthesized theophylline (TPH) complexes with ruthenium(III), platinum(IV), and iridium(III) metal ions. The metal ions indicated above were found to align with the TPH drug chelate as a mono-dentate ligand *via* the deprotonated NH group at the nitrogen atom position N7, as verified by FTIR measurements. Additionally, the complexes conductivity and magnetic susceptibility were examined. The octahedral geometry for the synthesized complexes was proposed by the current data. Except for the iridium(III) complex, which has a non-electrolytic nature due to the presence of a chlorine atom inside the chelation sphere, the molar conductivity of the complexes in DMSO solution was electrolyte in nature. Theophylline complexes with a (metal: ligand) stoichiometry of 1:2 were produced. The TPH complexes have also been tested *in vitro* against G(+) bacteria (*Bacillus subtilis* and *Staphylococcus Aureus*) and G(-) bacteria (*Pseudomonas aeruginosa* and *Escherichia coli*) to evaluate their antibacterial efficacy. Human breast and liver cancer cell lines were used as a test for the TPH complexes *in vitro* anti-cancer properties.

KEY WORDS: Theophylline, Metal ions, Chelation, Octahedral, Spectral analysis, Nano-particles, Biological evaluation

INTRODUCTION

Purine bases are heterocyclic bases that are nitrogen-containing and play a vital role in nucleic acids' physiological activity [1, 2]. In the domains of pharmacology and physiology, they represent a significant class of anti-inflammatory and anticancer drugs [3]. Their ability to influence alterations in fundamental cellular processes is what gives them their anti-inflammatory properties. These substances function as phosphodiesterase's competitive inhibitors, deactivating cyclic 3,5-adenosine monophosphate (3,5-c AMP). The inhibition of an enzyme leads to the activation of 3,5-c AMP, which in turn drives the promotion of cellular activities and glycogenolysis. Additionally, it has been suggested that the purine medicines work by lessening the binding of calcium in the cell's membrane and myoplasm, which in turn affects the muscles' ability to contract [4, 5].

One significant member of the class of purine bases that belongs to the anti-inflammatory medicines is theophylline (1,3-dimethyl-xanthine) [6]. It is widely recognized for its hydrotropic properties and for its capacity to solubilize a broad range of medicinal substances [3]. As a result, it is frequently prescribed as a medication to treat conditions affecting the physiological processes of the respiratory system, including asthma or COPD [7, 8]. Theophylline was demonstrated to cause apoptosis and reduce cell growth in HeLa and MCF-7 breast cancer cell lines, but not in MCF-10A, a normal human breast cell line. It was also reported to exhibit cytotoxic effect against the MDA-MB-231 human breast cancer cell line [3, 4]. The observed effects in both investigations

*Corresponding author. E-mail: moamen@tu.edu.sa ; msrefat@yahoo.com

were observed at IC_{50} values much higher above the safe therapeutic range of theophylline, at >1 mM (>0.18 g/L) [9-11]. A novel cancer medication would also be administered at an IC_{99} concentration to attain a high cell death rather than an IC_{50} concentration, which would leave 50% of cells surviving, if it were to be utilized therapeutically. Due to its limited therapeutic index and cardiotoxic effects, theophylline should be used with extreme caution as a stand-alone anti-cancer drug [12]. Because of this, there has been a lot of interest in creating model complexes with theophylline to enhance its anti-cancer potential, as several metal complexes have antitumor action. This might resemble how metal ions interact with DNA [13, 14].

Through N and/or O donor atoms, theophylline coordinates with metal ions. It coordinates metal ions through the N7 atom and acts as a monodentate ligand in neutral or basic environments [15-17]. It can act as a bridging ligand with simultaneous N(7)/O(6) chelation and N(9) coordination in some situations, or as a bidentate N(7)/O(6) chelating ligand in others. N(7) becomes protonated at pH < 5, and theophylline uses N(9) to coordinate metals [9, 18-20]. Conversely, linked methyl groups prevented N(1) and N(3) atoms from interacting with metal ions [3]. Theophylline typically exhibits a mono coordination mode with first row transitional metals like cobalt(II), manganese(II), zinc (II), iron(II), and nickel(II) through the imidazole ring's N(7) atom under basic or neutral circumstances [1, 18].

Despite the fact that theophylline-metal complexes are important in the realms of biology and medicine, no papers have been published that examine the antibacterial and anticancer properties of theophylline in conjunction with biologically interesting metals like Pt(IV), Ru(III), and Ir(III). Therefore, the goal of this work is to use various analytical techniques to explore the coordination chemistry of theophylline-Pt^{4+}, Ru^{3+}, Ir^{3+} complexes and evaluate their activities against various types of bacteria, fungus, and cancer cells.

EXPERIMENTAL

Chemicals

The theophylline medication, $RuCl_3$, $H_2PtCl_6.6H_2O$, and $IrCl_3.xH_2O$ salts (Sigma-Aldrich Chemical Corporation, St. Louis, MO, USA), together with all other analytical-grade chemicals and solvents, were used without additional purifications.

Synthesis of three new Ru^{3+}, pt^{4+}, and Ir^{3+} theophylline complexes

$[Ru(TP)_2(H_2O)_4].Cl$, $[Pt(TP)_2(H_2O)_4].Cl_2$, and *$[Ir(TP)_2(H_2O)_3(Cl)]$ complexes*. A solutions of 1.0 mmol ($RuCl_3$, $H_2PtCl_6.6H_2O$, and $IrCl_3.xH_2O$) and 2.0 mmol theophylline were combined with 25 mL of methanol, refluxed for two hours, and then neutralized with NH_4OH at a pH of around 8.

Instrumentals

With the Perkin Elmer CHN 2400 (USA), elemental studies of the concentrations of carbon, hydrogen, nitrogen, and chlorine were carried out. Using a Jenway 4010 conductivity meter, the molar conductivities of newly made 1.0×10^{-3} mol/cm^3 dimethyl sulfoxide (DMSO) solutions were determined for the dissolved chemicals. Using a Bruker FTIR Spectrophotometer, the infrared spectra were captured (4000–400 cm^{-1}). A UV2 Unicam UV/Vis Spectrophotometer equipped with a quartz cell with a 1.0 cm path length was used to record the UV-Vis absorption spectra in DMSO solvent within the 800-200 nm range. The Magnetic Susceptibility Balance from Sherwood Scientific, located at Cambridge Science Park, Cambridge, England, was used to calculate magnetic moments at a temperature of 25 ºC. A Bruker 600 MHz spectrometer was used to record ^{1}H-NMR spectra in DMSO solutions, with TMS serving as the internal standard. Using a Shimadzu thermo-gravimetric analyzer, the TG/DTG-50H thermal investigations were conducted under nitrogen up to 800 ºC. The X 'Pert PRO PANanalytical X-ray powder diffraction, target copper with secondary monochromate, was used to record the X-ray diffraction patterns. JEOL 100s microscopy was used to capture the pictures from the transmission electron microscopy (TEM).

Biological evaluations

A modified Kirby-Bauer disc diffusion method was used to assess the antimicrobial activity of the tested materials [21]. In summary, 10 millilitres of fresh media were used to cultivate 100 microliters of G(+) bacteria (*Bacillus subtilis* and *Staphylococcus Aureus*) and G(-) bacteria (*Pseudomonas aeruginosa* and *Escherichia coli*) until the bacteria attained a count of roughly 108 cells/mL. On agar plates that corresponded to the broth in which they were kept, 100 µL of the microbial suspension was dispersed. The disc diffusion method should be used to screen for susceptibility in isolated colonies of any organism that may be pathogenic [21]. These colonies should be selected from primary agar plates.

To evaluate whether or not Ru^{3+}, pt^{4+}, and Ir^{3+} theophylline complexes exhibit a tumor cell killing ability, the effect of DMSO-soluble Ru^{3+}, pt^{4+}, and Ir^{3+} theophylline complexes on human breast cancer (MCF-7) and the human hepatocellular carcinoma (HepG-2) cell lines were investigated. The two cell lines were propagated in Dulbecco's modified Eagle's medium (DMEM) supplemented with 10% heat-inactivated fetal bovine serum, 1% L-glutamine, HEPES buffer and 50 µg/mL gentamycin. All cells were maintained at 37 ºC in a humidified atmosphere with 5% CO_2 and were subcultures two times a week. The effect of treatment with Ru^{3+}, pt^{4+}, and Ir^{3+} theophylline complexes on the survival of the two human tumor cell lines was assessed using a viability assay in distilled water [22, 23]. Cells were seeded in 96-well plates at 1×10^4 cells/well. Three wells were used for each concentration of the test sample. Control cells were incubated without test sample and with or without DMSO. The little percentage of DMSO present in the wells (maximal 0.1%) was found not to affect the experiment. After incubation of the cells for at 37 °C, various concentrations of sample were added, and the incubation was continued for 24 h and viable cells yield was determined by a colorimetric method. Treated samples were compared with the cell control in the absence of the tested compounds. All experiments were carried out in triplicate. The cell cytotoxic effect of each tested compound was calculated. The optical density was measured with the microplate reader (SunRise, TECAN, Inc, USA) to determine the number of viable cells and the percentage of viability was calculated as [1-(ODt/ODc)]×100% where ODt is the mean optical density of wells treated with the tested sample and ODc is the mean optical density of untreated cells. The relation between surviving cells and drug concentration is plotted to get the survival curve of each tumor cell line after treatment with the specified compound. The 50% inhibitory concentration (IC_{50}), the concentration required to cause toxic effects in 50% of intact cells, was estimated from graphic plots of the dose response curve for each conc. using Graphpad Prism software (San Diego, CA. USA).

RESULTS AND DISCUSSION

Results of stoichiometric and molar conductance

The elemental analyses show that there is good agreement between estimated and experimental results for the Ru(III), Pt(IV), and Ir(III) theophylline complexes. The colors of the complexes of ruthenium(III), platinum(IV), and iridium(III) are dark brown, yellowish brown, and black. It was discovered that the complexes were soluble in DMSO and DMF solvents but insoluble in ether, water, methanol, ethanol, chloroform, and ester. The Ru^{3+}, pt^{4+}, and Ir^{3+} theophylline complexes broke down at a temperature between 376 and 550 ºC. This section includes a summary of the analytical results for these complexes as well as some physico-chemical properties of the Ru^{3+}, pt^{4+}, and Ir^{3+} theophylline complexes. Theophylline (TPH) ligand and metal ions Ru^{3+}, pt^{4+}, and Ir^{3+} interacted in 1:2 molar proportions (metal-to-ligand), according to the analytical data. With the exception of the iridium(III) complex, which has a non-electrolytic statement at Λ_M = 17 $\Omega^{-1}.cm^2.mol^{-1}$ [24], conductance measurements for ruthenium(III) and platinum(IV) complexes in 10^{-3} M dimethyl sulfoxide solution show electrolytes behavior. This suggests that one or two chlorine atoms are present outside the coordination sphere for the ruthenium(III) and platinum(IV) complexes, respectively. Through the use of gravimetric analysis, the metal contents are estimated. The infrared and ultraviolet-visible spectra of Ru^{3+}, pt^{4+}, and Ir^{3+} theophylline complexes are examined, along with tabulations and possible assignments of their several significant distinctive bands.

$[Ru(TP)_2(H_2O)_4].Cl$ complex resulted in a dark brown precipitate, yield 73%. Dec. temp., 376 °C. Anal. (Calc.) Found, %: C, (29.63) 29.54; H; (3.88) 3.72; N, (19.76) 19.65; Cl, (6.26) 6.19.

$[Pt(TP)_2(H_2O)_4].Cl_2$ complex produced with a yellowish brown in color, yield 75%. Dec. temp., 550 °C. Anal. (Calc.) Found, %: C, (24.12) 24.10; H; (3.16) 3.09; N, (16.08) 15.96; Cl, (5.10) 5.04.

$[Ir(TP)_2(H_2O)_3(Cl)]$ complex has a black precipitate, yield 71%. Dec. temp., 391 °C. Anal. (Calc.) Found, %: C, (26.25) 26.17; H; (3.12) 3.08; N, (17.50) 17.43; Cl, (5.55) 5.51.

Assignments of infrared spectra

Figure 1 displays the infrared spectra of the Ru(III), Pt(IV), and Ir(III) complexes of theophylline free donor. Table 1 lists the peaks of several significant vibrational modes that were seen in the TPH and their complexes spectra for comparison. When it comes to theophylline complexes, the ligand can chelate with the metal ion either by using N(7) of the –NH five member of the imidazole ring or by using the oxygen atom of carbonyl linked to C(6) [25-29]. The TPH free ligand exhibits a distinct band in its infrared spectra at 3120 cm^{-1}, which is indicative of the stretching vibration of ν(N7-H).

In the instance of a free ligand, the three stretching frequencies that were detected at 1720, 1665, and 1564 cm^{-1} were ascribed to ν(C=O), ν(C=C) and ν(C=N), respectively. Since the peaks of ν(C=O), ν(C=C), and ν(C=N) on chelation appeared at roughly the same wavenumbers of free TPH ligand, the interaction of carbonyl at C(6) or nitrogen at N(9) with Ru(III), Pt(IV), and Ir(III) metal ions cannot be the cause of this result, as indicated by the electronic spectra of these complexes.

Furthermore, the imidazole ring nitrogen N(7) of theophylline is deprotonated and its N(7) atom is coordinated to the metal ion, as indicated by the band's absence at 3120 cm^{-1} due to ν(N–H) stretching in the complexes. The majority of the theophyllinato complexes reported in the literature also contain this coordination site [1, 3, 5, 9]. The bands present at around 448 and 420 cm^{-1} in the IR spectra range within 1000-400 cm^{-1} of all the Ru(III), Pt(IV), and Ir(III) theophylline complexes were attributed to the ν(M-N) stretching frequency.

Table 1. FTIR assignments (cm^{-1}) of theophylline complexes.

Compounds	ν(N_7-H)	ν(C_6=O)	ν(C=C)	ν(C=N)	ν(M-N)
TPE	3120	1720	1665	1564	-
Ru(III) complex	-	1710	1638	1548	448, 423
Pt(IV) complex	-	1704	1653	1552	448, 418
Ir(III) complex	-	1714	1663	1557	448, 419

A B

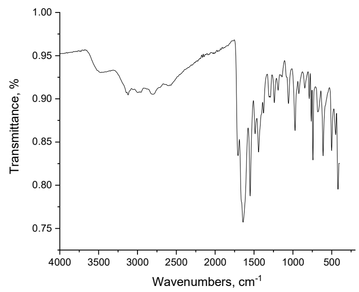

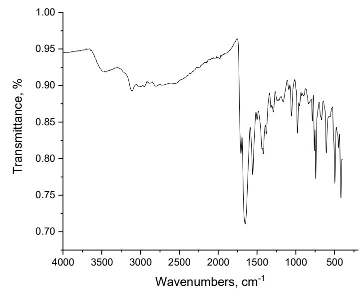

C

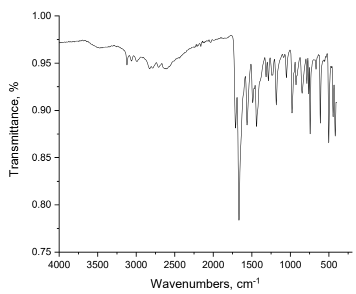

Figure 1. FTIR spectra of (A): Ru(III), (B): Pt(IV), and (C): Ir(III) theophylline complexes.

Magnetic and electronic measurements

Two absorption maxima, corresponding to π-π* and n-π* transitions, are visible in the electronic spectrum of the theophylline drug at 275 and 289 nm. The carbonyl group's n-π* transition, which is responsible for the band in the theophylline's electronic spectrum at 289 nm, remained nearly unaltered upon complexation, indicating that the carbonyl group of the TPH ligand was not involved in complexation [30]. The Ru(III) complex exhibits three electronic transitions at 498 nm, 425 nm, and 360 nm. These transitions can be explained by $^2T_{2g}\rightarrow{}^4T_{1g}$ (ν1), $^2T_{2g}\rightarrow{}^4T_{2g}$ (ν2), and $^2T_{2g}\rightarrow{}^2A_{2g}$ (ν3). The magnetic moment of 1.87 B.M. of the ruthenium(III) complex supports the observation of a single unpaired electron in an octahedral environment for the Ru(III) ion in a low spin $4d^5$ configuration [31-34]. The different bands of platinum(IV) theophylline complex at 287 nm and 337 nm can be explained by metal ligand charge transfer (M→LCT) and the d-d transition band. N→Pt(IV) metal charge transfer ($L\pi\rightarrow Pt_{CT}$) and d-d transition bands combine to form the other band at 419 [34]. The UV–Vis spectrum of iridium(III) complex shows two bands at 339 nm and 288 nm, which were deduced from the ground state $^1A_{1g}$. The two transitions that were allowed by spin, $^1A_{1g}\rightarrow{}^1T_{1g}$ (ν1) and $^1A_{1g}\rightarrow{}^1T_{2g}$ (ν2), were found to be within the expected ranges [27-31]. Two MLCT-related absorption peaks at 433 and 500 nm were visible in the Ir(III) complex spectrum. Given that the complexes of iridium(III) and platinum(IV) exhibit diamagnetic characteristics, their geometries must be octahedral.

[1]H NMR study

Figure 2 illustrates the scanning of the platinum(IV) complex's ^{1}H-NMR data. When complexation occurs in theophylline (Formula 1), the broad peak attributed to N7H (δ = 14) disappears, indicating that the deprotonated hydrogen atom of the NH group is involved (Figure 3). Due to the ligand's altered electronic environment upon complexation, the peaks receive an insignificant downfield shift (Table 2).

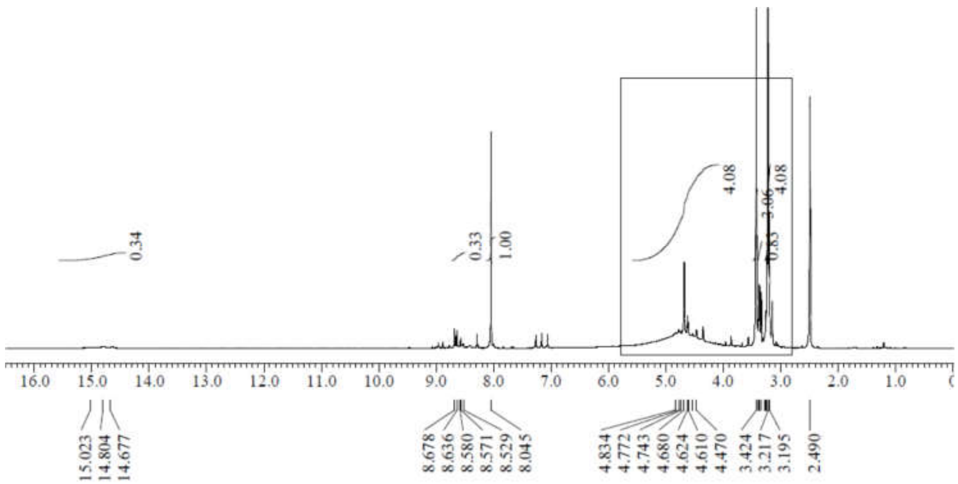

Figure 2. ^{1}H-NMR spectrum of Pt(IV) theophylline complex.

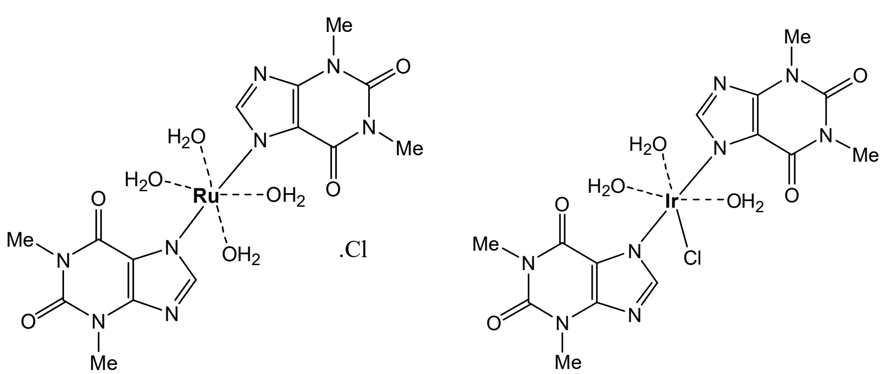

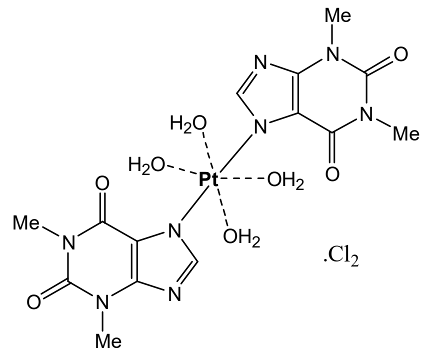

Figure 3. Speculated structures of Ru^{III}, Pt^{IV} and Ir^{III} theophylline complexes.

Table 2. ^{1}H-NMR proton signals of the TPH ligand and Pt(IV) complex.

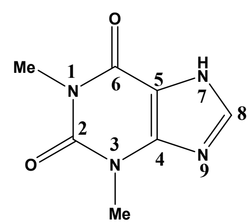

$\delta^{1}H$	N(7)-H	C(8)-H	N(3)-CH_3	N(1)-CH_3
TPH	14	7.975	3.200	3.400
Pt(IV)	-	8.580	3.217	3.424

Morphological investigations (XRD and TEM)

The X-ray diffraction patterns of the theophyllinato complexes of ruthenium(III), platinum(IV), and iridium(III) exhibit a crystalline-to-amorphous behavior, as illustrated in Figures 4A-C. Using the Debye-Scherrer equation [35], the average crystallite sizes of the theophyllinato complexes are calculated at the peak width at half height of the most intense peak (FWHM) at 2θ (Table 3). In a given material, the dislocation density is inversely related to the size of the crystallites and directly proportional to the lattice strain. A decrease in both strain and dislocation density signifies the creation of high-quality complexes [36]. The dislocation density (δ) in Table 3 represents the dislocation network in theophyllinato complexes.

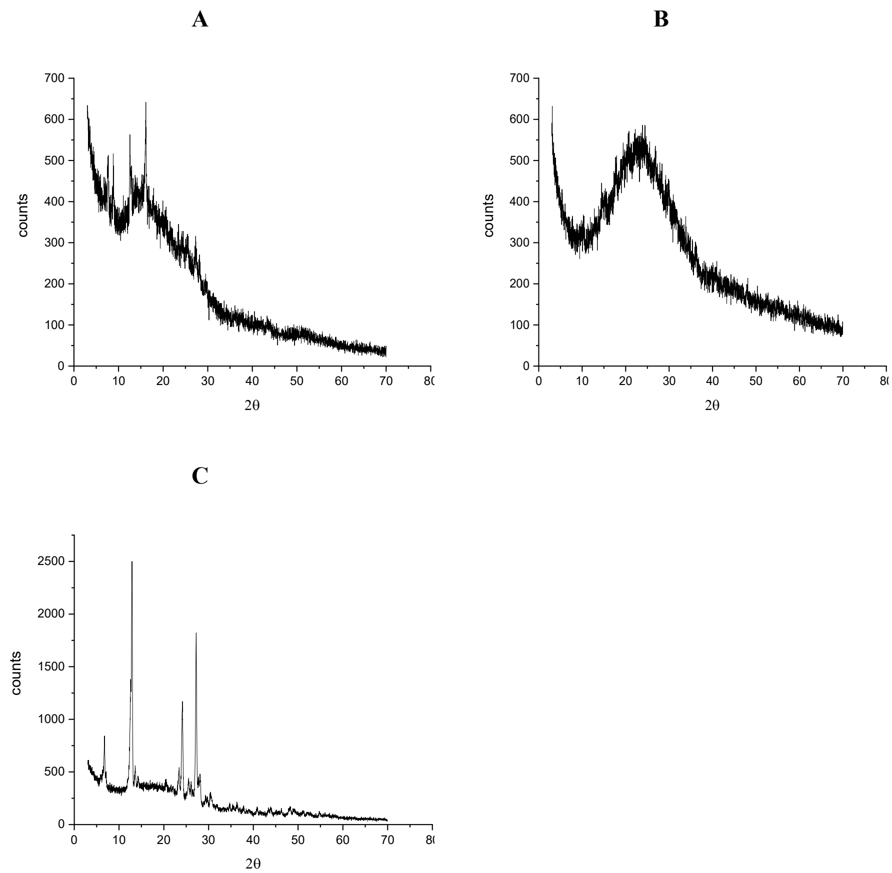

Figure 4. XRD spectra of (A): Ru(III), (B): Pt(IV), and (C): Ir(III) theophylline complexes.

Table 3. Physical spectral calculations of theophyllinato complexes of Ru(III), Pt(IV), and Ir(III).

Complexes	2θ	Intensity	d-pacing	D (nm)	δ (10^{12}.lin.m^{-2})
Ru(III)	16	100	5.4902	43	0.0005
Pt(IV)	24	100	3.6352	9	0.0123
Ir(III)	13	100	6.8708	27	0.0014

The nanoscale particles in the theophyllinato complexes of Ru(III), Pt(IV), and Ir(III) are visible in the TEM micrographs (Figure 5A-C). Theophylline complexes' average particle diameter was calculated by fitting the data derived from TEM images to a normal distribution. Particle sizes ranged from 10 to 40 nm, according to the generated photos. The TEM micrographs (Figure 5A-C) show a black area that varies in size and has spherical forms.

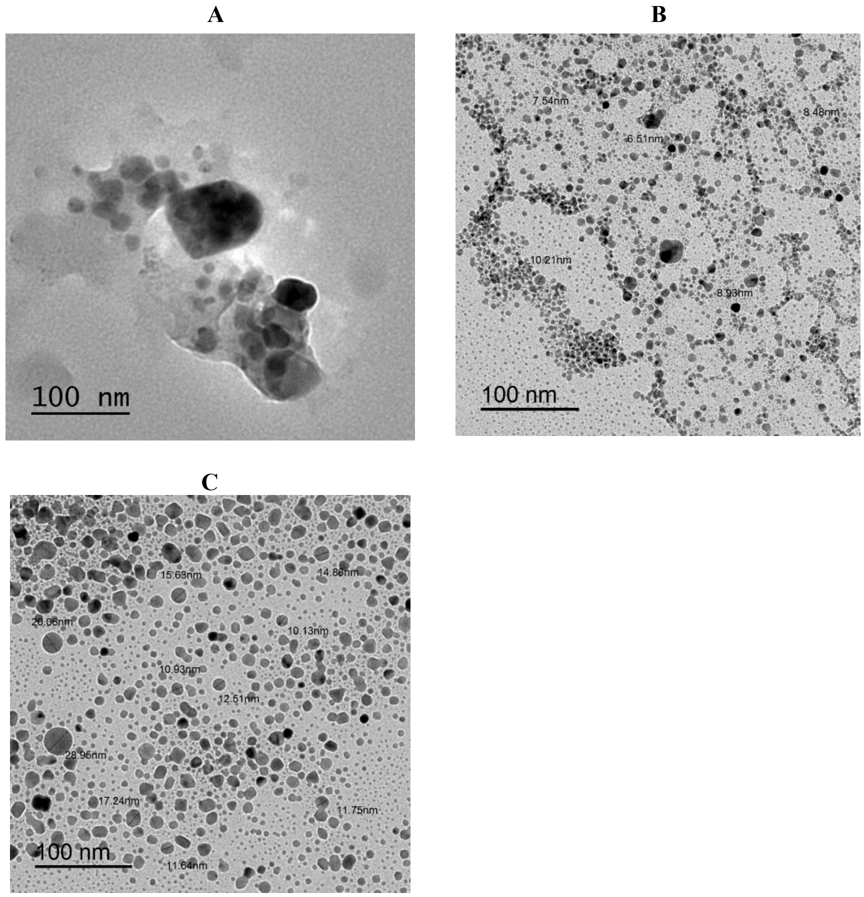

Figure 5. TEM images of (A): Ru(III), (B): Pt(IV), and (C): Ir(III) theophylline complexes.

Thermogravimetric analyses

Based on the TGA-DrTGA-DSC curves (Figure 6A-C), thermogravimetric studies of the theophyllinato complexes of Ru(III), Pt(IV), and Ir(III) have been addressed. Ru(III), Pt(IV), and Ir(III) anhydrous theophyllinato complexes are stable at 200 ºC. At thermo gravimetric maximum peaks DTG_{max} = (150, 290, 375, 510, and 660 ºC), (140, 250, 350, 550, and 575 ºC), and (325, 400, and 490 ºC), respectively, the TGA-DrTGA-DSC curves of the Ru(III), Pt(IV), and Ir(III) complexes demonstrate a thermal decomposition in three to five degradation steps. These endothermic peaks correspond to the pyrolysis of the two theophylline moieties, coordinated water molecules, and chlorine atoms. RuO_2, PtO, and IrO_2 are represented by the residual weights at these DTG_{max} points, which are 24.22, 27.51, and 32.21% of the initial weight.

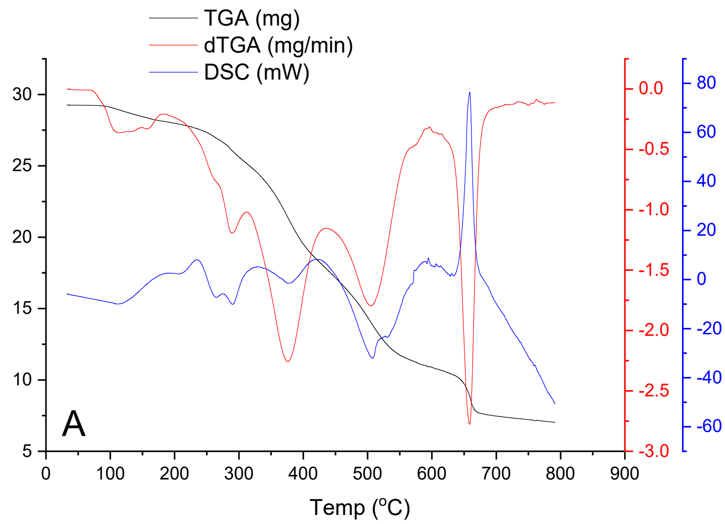

Figure 6A. TGA, dTGA, and DSC curves of Ru(III)-TP complex.

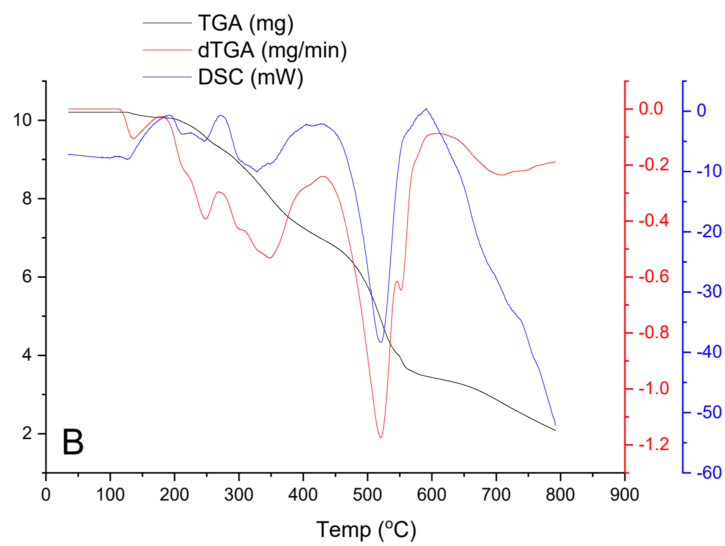

Figure 6B. TGA, dTGA, and DSC curves of Pt(IV)-TP complex.

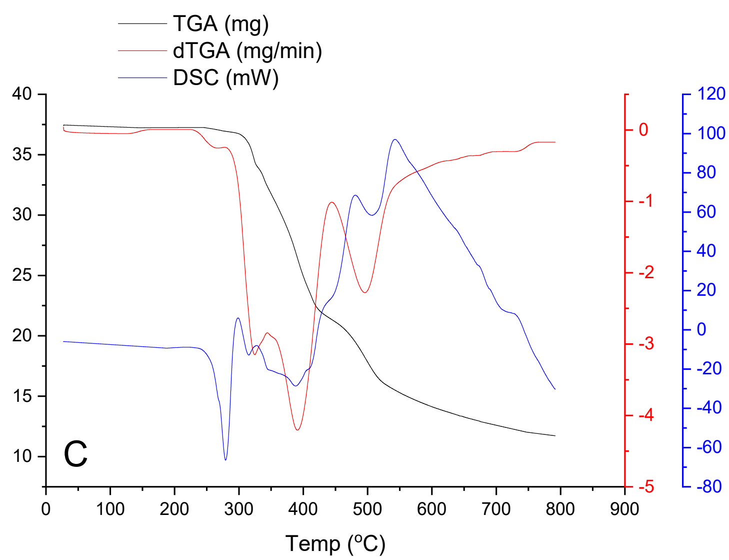

Figure 6C. TGA, dTGA, and DSC curves of Ir(III)-TP complex.

Evaluations of antimicrobial and anticancer activities

The antibacterial properties of the Ru(III), Pt(IV), and Ir(III) theophyllinato complexes have been evaluated in vitro against G(+) bacteria, such as *Bacillus subtilis* and *Staphylococcus Aureus*, and G(-) bacteria, such as *Pseudomonas aeruginosa* and *Escherichia coli*. Table 4 provides a summary of the zones of inhibition generated by the test substances. It has been noted that: (i) Compared to free TPH medication, the ruthenium (III) and iridium (III) complexes effectively inhibit *Bacillus subtilis* and *Escherichia coli*. (ii) Compared to free TPE medication, the platinum (IV) complex effectively inhibits G(+) bacteria (*Bacillus subtilis* and *Staphylococcus Aureus*) and G(-) bacteria (*Pseudomonas aeruginosa* and *Escherichia coli*).

Because of the ligand orbital overlap and partial sharing of the metal ion's positive charge with donor groups during chelation, the polarity of the metal ion is lowered to a higher extent. Moreover, it improves the complex's lipophilicity and raises the delocalization of -electrons throughout the entire chelate ring. The enhanced lipophilicity facilitates the complexes' entry into lipid membranes and prevents the metal binding sites on the microorganism's enzymes. However, due to their toxicity and propensity to bind to free ligands found in biological systems like the nitrogen bases of proteins and nucleic acids, metal salts alone do not function as effective antibacterial agents despite having higher activity than the complexes under investigation [37, 38].

In *vitro* cytotoxicity assessment of the Ru(III), Pt(IV), and Ir(III) theophyllinato complexes were performed on human breast (MCF-7) and liver (HepG-2) tumor cell lines. The results evaluated upon the determination of inhibitory concentration of 50 % (IC_{50}), the data was shown in (Figure 1S, supplementary material). The evaluation of cytotoxicity of Ir(III) (IC_{50} = 50.5 ± 3.2 µg/mL), Pt(IV) (IC_{50} = 114 ± 5.4 µg/mL), Ru(III)-TPH (IC_{50} = 47 ± 3.1 µg/mL) theophyllinato complexes against HepG-2 cell line. Evaluation of cytotoxicity of Ir(III) (IC_{50} = 57.60 ± 3.8 µg/mL), Pt(IV) (IC_{50} = 135 ± 6.2 µg/mL), Ru(III)-TPH (IC_{50} = 55 ± 3.4 µg/mL) theophyllinato complexes against MCF-7 cell line.

Table 4. Inhibition zone diameter of theophyllinato complexes against some kind of bacteria.

Sample	Inhibition zone diameter (mm/mg sample)			
	Bacterial species			
	G^+		G^-	
	Bacillus subtilis	*Staphylococcus aureus*	*Escherichia coli*	*Pseudomonas aeruginosa*
Control: DMSO	0.0	0.0	0.0	0.0
Standard: Ampicillin Antibacterial agent	26	21	25	26
TPH ligand	6	12	7	12
Ir(III)-TP complex	9	9	9	9
Pt(IV)-TP complex	16	19	16	17
Ru(III)-TP complex	12	12	11	12

- G: Gram reaction. Solvent: DMSO.

CONCLUSION

In the present paper, we are describing three of transition metal complexes of theophylline with Ru(III), Pt(IV), and Ir(III). These complexes were characterized by elemental analysis, molar conductance, IR, NMR, magnetic susceptibility, UV-visible spectral studies, SEM, TEM and X-ray diffraction. Based on the above studies, the ligand behaves as monodentate N donor and forms coordinate bonds through deprotonated NH group at the nitrogen atom position N7 in five-member ring. The complexes of $[Ru(TP)_2(H_2O)_4].Cl$ and $[Pt(TP)_2(H_2O)_4].Cl_2$, were found to electrolytic nature but the $[Ir(TP)_2(H_2O)_3(Cl)]$ complex has a non-electrolytic nature on the basis of values of molar conductance. Analytical data and stoichiometry suggest ligand metal ratio of 2:1 for all the complexes. Electronic spectra and Magnetic susceptibility measurements reveal octahedral geometry for Ru(III), Pt(IV), and Ir(III) complexes. The synthesized metal complexes have been screened for their antibacterial (*Bacillus subtilis*, *Staphylococcus Aureus*, *Pseudomonas aeruginosa* and *Escherichia coli*) and anti-cancer activities against human breast (MCF-7) and liver (HepG-2) tumor cell lines.

ACKNOWLEDGEMENT

Princess Nourah bint Abdulrahman University Researchers Supporting Project number (PNURSP2024R75), Princess Nourah bint Abdulrahman University, Riyadh, Saudi Arabia.

REFERENCES

1. Gacki, M.; Kafarska, K.; Pietrzak, A.; Korona-Glowniak, I.; Wolf, W.M. Synthesis, characterization, crystal structure and biological activity of metal(II) complexes with theophylline. *J. Saudi Chem. Soc.* **2019**, 23, 346-354.
2. Abd El-Wahab, Z.H. Complexation of 4-amino-1,3 dimethyl-2,6 pyrimidine-dione derivatives with cobalt(II) and nickel(II)ions: synthesis, spectral, thermal and antimicrobial studies. *J. Coord. Chem.* **2008**, 61, 1696-1709.
3. Altun, Ö.; Şuözer, M. Synthesis, spectral analysis, stability constants, antioxidant and biological activities of Co(II), Ni(II) and Cu(II) mixed ligand complexes of nicotinamide, theophylline and thiocyanate. *J. Mol. Struct.* **2017**, 1149, 307-314.
4. Grollman, A.; Grollman, E.F. *Pharmacology and Therapeutics*, Lea and Febiger: Philadelphia; **1970**; p. 192.
5. Marwaha, S.S.; Kaur, J.; Sodhi, G.S. Structure determination and anti-inflammatory activity of some purine complexes. *Metal-Based Drugs* **1995**, 2, 13-17.

6. Novena, L.M.; Kumar, S.S.; Athimoolam, S.; Saminathan, K.; Sridhar, B. Single crystal, vibrational and computational studies of theophylline (a bronchodilator drug) and its chloride salt. *J. Mol. Struct.* **2017**, 1133, 294-306.
7. Santos, C.I.A.V.; Ramos, M.L.; Justino, L.L.G.; Burrows, H.D.; Valente, A.J.M.; Esteso, M.A.; Leaist, D.G.; Ribeiro, A.C.F. Effect of pH in the structure and mass transport by diffusion of theophylline. *J. Chem. Thermodyn*. **2017**, 110, 162-170.
8. Ruddarraju, R.R.; Murugulla, A.C.; Kotla, R.; Chandra, M.; Tirumalasetty, B.; Wudayagiri, R.; Donthabakthuni, S.; Maroju, R.; Baburao, K.; Parasa, L.S. Design, synthesis, anticancer, antimicrobial activities and molecular docking studies of theophylline containing acetylenes and theophylline containing 1,2,3-triazoles with variant nucleoside derivatives. *Eur. J. Med. Chem*. **2016**, 123, 379-396.
9. Gordon, A.T.; Abosede, O.O.; Ntsimango, S.; Hosten, E.C.; Myeza, N.; van Eyk, A.; Harmse, L.; Ogunlaja, A.S. Synthesis and anticancer evaluation of copper(II)-and manganese(II)-theophylline mixed ligand complexes. *Polyhedron* **2022**, 214, 115649.
10. Bombicz, P.; Madarász, J.; Forizs, E.; Foch, I. Structure and thermal behaviour of (SPY-5-12)-(2-aminoethanol-N)(2-aminoethanol-N, O)-bis (theophyllinato) copper(II) dihydrate: A model for DNA-metal interactions. *Polyhedron* **1997**, 16, 3601-3607.
11. Forizs, E.; David, L.; Cozar, O.; Chiş, V.; Damian, G.; Csibi, J. IR and ESR studies on novel Cu(II) theophyllinato complexes containing mono-or bidentate ligands. *J. Mol. Struct.* **1999**, 482, 143-147.
12. Singh, N.K.; Kumbhar, A.A.; Pokharel, Y.R.; Yadav, P.N. Anticancer potency of copper(II) complexes of thiosemicarbazones. *J. Inorg. Biochem.* **2020**, 210, 111134.
13. Alam, N.; Islam, M.; Najnin, H.; Shakya, S.; Khan, I.M.; Hossain, M.W.; Zaidi, R.; Design and characterization of a binary CT complex of imidazole-oxyresveratrol: Exploring its pharmacological and computational aspects. *J. Biomol. Struct. Dyn.* **2024**, 42, 1319-1335.
14. Hamaamin, H.N.; Hameed, H.A.; Jamalis, J.; Shakya, S.; Chander, S.; Kharkwal, H.; Murugesan, S.; Ajit, B.V.; Gupta, P. Potential inhibitory activity of phytoconstituents against black fungus: In silico ADMET, molecular docking and MD simulation studies. *Comput Toxicol*. **2022**, 24, 100247.
15. Abdulah, H.I.; Hussain, D.H.; Rheima, A.M. Synthesis of α-Fe_2O_3, γ-Fe_2O_3 and Fe_3O_4 nanoparticles by electrochemical method. *J. Chem. Biol. Phys. Sci. (JCBPS)* **2016**, 6, 1288-1296
16. Ismail, A.H.; Al-Bairmani, H.K.; Abbas, Z.S.; Rheima, A.M. Nanoscale synthesis of metal(II) theophylline complexes and assessment of their biological activity. *Nano Biomed. Eng*. **2020**, 12, 139-147.
17. Kistenmacher, T.J.; Szalda, D.J.; Marzilli, L.G. Intercalative stacking interactions and interligand hydrogen bonding in metal purine complexes. Crystal and molecular structure of (N-salicylidene-methylethylenediamine)(theophyllinato)copper(II) monohydrate. *Inorg. Chem*. **1975**, 14, 1686-1691.
18. Aoki, K.; Yamazaki, H. Interaction of tetrakis(-m-carboxylato) dirhodiurn(II), an antitumour agent, with nucleic acid bases. X-ray crystal structures of [Rh_2(acetato)$_4$(theophylline)$_2$] and[Rh_2(acetato)$_4$(caffeine)$_2$]. *J.C.S. Chem. Commun*. **1980**, 926, 186-188.
19. Griffith, E.H.; Amma, E.L. Reaction of $PtCl_4^-$ with theophylline: X-ray crystal structures of bis(theophyllinum) tetrachloroplatine(II) and theophyllinum trichlorotheophyllineplatinate(II). *Inorg. Chem*. **1979**, 7, 322-324.
20. Ismail, A.H.; Al-Bairmani, H.K.; Abbas, Z.S.; Rheima, A.M. Synthesis, characterization, spectroscopic and biological studies of Zn(II), Mn(II) and Fe(II) theophylline complexes in nanoscale. *Nano Biomed. Eng.* **2020**, 12, 253-261.
21. Bauer, A.W.; Kirby, W.A.; Sherris, C.; Turck, M. Antibiotic susceptibility testing by a standardized single disk method. *Am. J. Clin. Pathol.* **1996**, 45, 493-496.

22. Mosmann, T. Rapid colorimetric assay for cellular growth and survival: Application to proliferation and cytotoxicity assays. *J. Immunol. Methods* **1983**, 65, 55-63.
23. Gomha, S.M.; Riyadh, S.M.; Mahmmoud, E.A.; Elaasser, M.M. Synthesis and anticancer activities of thiazoles, 1,3-thiazines, and thiazolidine using chitosan-grafted-poly(vinylpyridine) as basic catalyst. *Heterocycles* **2015**, 91, 1227-1243.
24. Refat, M.S. Complexes of uranyl(II), vanadyl(II) and zirconyl(II) with orotic acid "vitamin B13": Synthesis, spectroscopic, thermal studies and antibacterial activity. *J. Mol. Struct*. **2007**, 842, 24-37.
25. El-Habeeb, A.A.; Refat, M.S. Three new complexes of theophylline drug Sc^{III}, Nb^{V} and W^{VI} ions: Spectroscopic, thermal stability, and antimicrobial studies. *Russ. J. Gen. Chem*. **2018**, 88, 2170-2176.
26. Refat, M.S. Synthesis, characterization, thermal and antimicrobial studies of diabetic drug models: Complexes of vanadyl(II) sulfate with ascorbic acid (vitamin C), riboflavin (vitamin B2) and nicotinamide (vitamin B3). *J. Mol. Struct*. **2010**, 969, 163-171.
27. Younes, A.A.O.; Saad, H.A.; Adam, A.M.A.; Alzoghibi, O.M.; Alsulaim, G.M.; Alsuhaibani, A.M.; Refat, M.S. Complexation of some alkaline earth metals with bidentate uracil ligand: Synthesis, spectroscopic and antimicrobial analysis. *Bull. Chem. Soc. Ethiop*. **2023**, 37, 945-957.
28. Alsuhaibani, A.M.; Adam, A.M.A.; Refat, M.S.; Kobeasy, M.I.; Bakare, S.B.; Bushara, E.S. Spectroscopic, thermal, and anticancer investigations of new cobalt(II) and nickel(II) triazine complexes. *Bull. Chem. Soc. Ethiop.* **2023**, 37, 1151-1162.
29. Almehizia, A.A.; Al-Omar, M.A.; Naglah, A.M.; Bhat, M.A.; Alanazi, F.S.; Alotaibi, F.A.; Refat, M.S.; Adam, A.M.A. Complexes of the antibiotic drug oxolinic acid with the Fe(III), Zn(II), Ca(II), and Mg(II) ions: Preparation, characterization, and in vitro evaluation of the biological activity. *Crystals* **2023**, 13, 1012.
30. Bhatia, S.; Kaushik, N.K.; Sodhi, G.S. Studies on organomercury(II) complexes of isoniacinamide. *Z. Naturforsch. B* **1988**, 43, 318-322.
31. Alghamdi, M.T.; Alsibaai, A.A.; Shahawi, M.S.; Refat, M.S. Structural and chelation behaviors of new Ru(III), Pt(IV) and Ir(III) gatifloxacin drug complexes: Spectroscopic characterizations. *J. Mol. Struct*. **2017**, 1130, 264-275.
32. Alibrahim, K.A.; Al-Saif, F.A.; Alghamdi, M.T.; El-Shahawi, M.S.; Moustafa, Y.M.; Refat, M.S. Synthesis, spectroscopic, thermal, antimicrobial and electrochemical characterization of some novel Ru(III), Pt(IV) and Ir(III) complexes of pipemidic acid. *RSC Adv.* **2018**, 8, 22515-22529.
33. Alibrahim, K.A.; Al-Saif, F.A.; Alghamdi, M.T.; El-Shahawi, M.S.; Althubeiti, K.; Aljuhani, E.; Refat, M.S. Spectroscopic, molecular structural, thermal, biological and voltammetric characterization of Ru^{3+}, Pt^{4+} and Ir^{3+} complexes of lomefloxacin drug. *Lat. Am. J. Pharm*. **2019**, 38, 1077-1090.
34. Lever, A.B. *Inorganic Electronic Spectroscopy*, Elsevier: Amsterdam; **1968**.
35. Klug, H.P. (Eds.) *X-ray Diffraction Procedures for Polycrystalline and Amorphous Materials*, Wiley: New York:, **1974**.
36. Velumani, S.; Mathew, X.; Sebastian, P.J. Structural and optical characterization of hot wall deposited CdSe*x*Te1−*x* films. *Solar Energy Mater. Solar Cells* **2003**, 76, 359-368.
37. Haergreaves, M.K.; Pritchard, J.G.; Dave, H.R. Cyclic carboxylic monoimides. *Chem. Res*. 1970, 70, 439-443.
38. Dharmaraj, N.; Viswanathamurthi, P.; Natarajan, K. Ruthenium(II) complexes containing bidentate Schiff bases and their antifungal activity. *Trans. Met. Chem*. **2001**, 26, 105-109.